Pb(II) and Mn(II) Supermolecular Polymers of Bipy and (4-Chlorophenyloxy) Acetate Anions: Syntheses, Structure and Fluorescence Properties

Long Li[a], Kaisheng Diao[a,b,*] and Yuqiu Ding[a]

[a]*College of Chemistry and Chemical Engineering, Guangxi University for Nationalities, Nanning 530006, People's Republic of China.*
[b]*Guangxi Key Laboratory of Chemistry and Engineering of Forest Products (Guangxi University for Nationalities), Nanning 530006, People's Republic of China.*

Received 17 September 2012, revised 7 November 2012, accepted 15 November 2012.

ABSTRACT

Two new supermolecular polymers of the formula $[Pb_4L_8(2,2'\text{-bipy})_4]$ 1 and $[MnL_2(4,4'\text{-bipy})]$ 2 [HL = (4-chlorophenyloxy)acetic acid] have been synthesized and characterized by X-ray single crystal diffraction analysis, elemental analysis, fluorescence spectroscopy method and electrochemical analysis. Complex 1 is a multinuclear dimmer in which four Pb ions are linked together by the L ligands. In complex 2, each carboxyl of L bridges two Mn ions to form infinite Mn–O–C-O rods. Both in complex 1 and complex 2, π–π stacking and van der Waals' interactions make the two complexes stable, 3-D, supermolecular polymers. This work will contribute to the design and synthesis of fluorescent, supramolecular polymers.

KEYWORDS

Supermolecular polymers, fluorescence, 4-chlorophenyloxyacetic acid.

1. Introduction

Halogen phenoxyl carboxylates, and auxin are widely used as agricultural pesticides [1–4]. However, they can also pollute the environment and result in the intoxication of animals and humans.[5] In order to decrease these bad effects, many researches have focused on the degradation of these pesticides.

Metal ion, self-assemblies of halogen phenoxyl carboxylates ligands have been studied for their structural characteristics, such as diverse coordination modes and conformations, and their potential applications as catalysts, luminescent, sorption, magnetic materials and biological reagents.[6–10] As bridging ligands, halogen phenoxyl carboxylates are of interest in the construction of polymeric coordination architectures, not only because of the fact that these polymers have a wide range of structural diversities and potential applications as porous materials and fluorescent materials, but also because these ligands exhibit rich coordination chemistry. (4-Chlorophenyloxy)acetic acid is a typical halogen phenoxyl carboxylate ligand. Many of the most interesting metal–organic polymers with one-, two- and three-dimensional networks have been engineered using anionic carboxylate ligands, and L in this work, possesses one flexible acetate.

This paper reports the synthesis, structure and fluorescence properties of two new supermolecular polymers, $[Pb_4L_8(2,2'\text{-bipy})_4]$ **1** and $[MnL_2(4,4'\text{-bipy})]$ **2**. The work will contribute to the design and synthesis of fluorescent materials, electrochemical materials, catalysts and other related fields.

In supermolecular construction, hydrogen bonding and van der Waals' forces are all important noncovalent interactions which determine the assembly of molecules and ions in solution, the gas phase, and the solid state.[11,12] Another important supermolecular force in molecular structure is π–π stacking, which can make complexes more stable. In particular, the π–π stacking interactions in solid state are widely observed in the construction of multi-dimensional structures in offset face-to-face and edge-to-face fashion.

*To whom correspondence should be addressed. E-mail: llgxmd@163.com

2. Experimental

2.1. Materials and Instrumentation

All reagents and solvents were used directly as supplied commercially without further purification. Elemental analysis for C, H, and N was carried out on a Perkin–Elmer 2400 II elemental analyzer. Excitation and emission spectra were acquired on a Perkin–Elmer instrument LS55 spectrofluorometer. Cyclic voltammetry was performed on a CHI760D electrochemical workstation. The three-electrode system consisted of a platinum wire counter electrode, a silver/silver chloride electrode, and a glassy carbon electrode (3.0 mm diameter) as working electrode. All electrochemical experiments were carried out in a conventional electrochemical cell holding methanol and water solution at room temperature.

2.2. Synthesis of the Complex $[Pb_4L_8(2,2'\text{-bipy})_4]$ 1

HL (279.7 mg, 1.5 mmol) and 2,2′-bipy (77 mg, 0.5 mmol) were dissolved a the mixture of 15 mL ethanol and 5 mL H_2O. To this, an aqueous solution of sodium hydroxide was added dropwise with stirring to adjust the pH value of the solution to 6. Subsequently, 10 mL aqueous solution of $Pb(C_2H_3O_2)_2{\cdot}3H_2O$ (189.6 mg, 0.5 mmol) was added. The mixture was continuously heated at 130 °C for three days. After cooling to room temperature, a lauter liquor was obtained. A small quantity of white precipitation in the reaction solution was removed by filtration. By slow evaporation of the lauter liquor at room temperature, after three days X-ray quality, colourless, block-shaped, single crystals were obtained. The crystals were isolated, washed with ethanol and dried at room temperature (Yield: 70 % based on Pb). Calcd. for

Table 1 Experimental data for complexes **1** and **2**.

Compound	**1**	**2**
Empirical formula	$C_{104}H_{80}Cl_8Pb_4N_8O_{24}$	$C_{26}H_{20}Cl_2MnN_2O_6$
Formula weight	2938.12	582.28
Crystal system	Triclinic	Monoclinic
Space group	P-1	C2/c
a (Å)	13.093(6)	22.838(12)
b (Å)	14.722(6)	11.679(5)
c (Å)	16.600(7)	9.720(4)
α (°)	93.426(7)	90
β (°)	112.626(6)	98.237(9)
γ(°)	112.939(6)	90
V(Å^3)	2635.8(19)	2566(2)
Z	1	4
D_c (mg m^{-3})	1.851	1.507
μ (mm^{-1})	6.647	0.767
F(000)	1416	1188
Crystal size (mm)	0.35 0.34 0.32	0.36 0.33 0.31
θ range	1.37–25.00	1.96–25.00
Reflections collected	14474	6778
Independent reflections	9171 [R(int) = 0.0514]	2256 [R(int) = 0.0272]
Completeness to θ = 25.00	0.987	1.000
Absorption correction	Multi-scan	Multi-scan
Max. and min. transmission	0.2249 and 0.2044	0.7969 and 0.7697
Data/restraints/parameters	9171/1089/667	2256/0/170
Goodness-of-fit on *F*	0.957	1.051
R indices [I > 2σ(I)]	R1 = 0.0554, wR2 = 0.1444	R1 = 0.0318, wR2 = 0.0782
R indices (all data)	R1 = 0.1007, wR2 = 0.1808	R1 = 0.0360, wR2 = 0.0810
Largest diff. features (eÅ^{-3})	1.876 and –1.598	0.199 and –0.334

$C_{104}H_{80}Cl_8Pb_4N_8O_{24}$: C 42.48, H 2.72, N 3.81 %. Found: C 42.47, H 2.72, N 3.82 %.

2.3. Synthesis of the Complex [MnL_2(4,4′-bipy)] 2

The synthesis of **2** was similar to that of **1** except that $MnCl_2 \cdot 4H_2O$ (97 mg, 0.5 mmol) and 4,4′-bipy (77 mg, 0.5 mmol) were used. Yellow, block-shaped, single crystals were obtained. The crystals were isolated, washed with ethanol and dried at room temperature (Yield: 65 % based on Mn). Calcd. for $C_{26}H_{20}Cl_2MnN_2O_6$: C 53.58, H 3.43, N 4.80 %. Found: C 53.57, H 3.43, N 4.80 %.

2.4. X-ray Data Collection and Structure Refinement

Crystallographic data were collected on a Bruker SMART CCD diffractometer with graphite monochromated Mo-Ka radiation (λ = 0.71073 Å) at T = 296 K. Absorption corrections were applied by using the multi-scan program.[13] The structure was solved by direct methods and successive Fourier difference syntheses (SHELXS-97). Anisotropic thermal parameters for all nonhydrogen atoms were refined anisotropically by full-matrix least-squares procedure against F^2 (SHELXL-97)[14]. Hydrogen atoms were set in calculated positions and refined by a riding mode, with a common thermal parameter. The crystallographic data and experimental details for the structure analysis are summarized in Table 1, and the selected bond lengths and angles are listed in Table 2.

3. Results and Discussion

3.1. Crystal Structure Descriptions

Single crystal X-ray analysis of **1** reveals that the asymmetric unit consists of two Pb(II) ions, two 2,2′-bipy and four L ligands. The Pb(II) ion in complex **1** has two different coordination numbers. Pb_1 coordinates to two nitrogen atoms, one from 2,2′-bipy (Pb_1–N 2.558(4)–2.581(4) Å) and five oxygen atoms from three different L ligands (Pb_1–O 2.558(4)–2.818(4)Å). Pb_2 coordinates to two nitrogen atoms, one from 2,2′-bipy (Pb_2–N 2.558(4)–2.565(4)Å) and six oxygen atoms from four L ligands (Pb_2–O 2.563(4)–2.925(4)Å), in which the Pb_2–O_4 and Pb_1–O_5 bond lengths are 2.929(5) and 2.817(5)Å, respectively These distances are much longer than Pb–O bond lengths in literature.[15–17] The L ligands, in complex **1**, offers three kinds of coordination modes (Scheme 1) to coordinate to four Pb ions altogether. This makes complex 1 a dimer. The environment of Pb is shown in in Fig. 1. There are many π-π stacking interactions in the crystal. The π-π stacking distances between two pyridine rings of different 2,2′-bipy ligands range from 3.779(4) to 4.095(4) Å, and their dihedral angles vary from 14.43(4) to 15.66 (4) °. These face to face π-π stacking interactions (Fig. 2) link the dimer in a 2-D, supermolecular, layer along the *ac*-plane (Fig. 3). π-π stacking interactions also exist between two benzene rings of L from different dimers (3.704(4) Å, 0.000(4) °), which connected these 2-D layers into a 3-D, supermolecular, structure (Fig. 4).

Table 2 The selected bond lengths (Å) and angles (°).

Complex **1**		Complex **2**	
Pb(1)-N(4)	2.559(11)	Mn(1)-O(2)#2	2.1322(15)
Pb(1)-O(8)	2.568(9)	Mn(1)-O(2)	2.1322(15)
Pb(1)-N(3)	2.576(10)	Mn(1)-O(3)	2.2008(16)
Pb(1)-O(10)	2.639(9)	Mn(1)-O(3)#2	2.2008(16)
Pb(1)-O(9)	2.654(10)	Mn(1)-N(1)	2.285(2)
Pb(1)-O(11)	2.719(9)	Mn(1)-N(2)#3	2.310(2)
Pb(1)-O(5)	2.817(9)	O(2)#2-Mn(1)-O(2)	171.74 (8)
Pb(2)-N(2)	2.555(10)	O(2)#2-Mn(1)-O(3)	84.35(6)
Pb(2)-N(1)	2.562(11)	O(2)-Mn(1)-O(3)	95.43(6)
Pb(2)-O(5)	2.565(8)	O(2)#2-Mn(1)-O(3)#2	95.43(6)
Pb(2)-O(3)	2.615(9)	O(3)-Mn(1)-O(3)#2	176.92(7)
Pb(2)-O(4)	2.786(9)	O(2)#2-Mn(1)-N(2)#3	94.13(4)
Pb(2)-O(8)	2.683(9)	O(3)#2-Mn(1)-N(2)#3	91.54(4)
Pb(2)-O(2)	2.710(9)	N(1)-Mn(1)-N(2)#3	180.000(1)
Pb(2)-O(4) #1	2.929(8)	O(2)#2-Mn(1)-N(1)	85.87(4)
N(4)-Pb(1)-O(8)	73.2(3)	O(3)-Mn(1)-N(1)	88.46(4)
N(4)-Pb(1)-N(3)	63.0(4)		
O(8)-Pb(1)-N(3)	84.3(3)		
O(8)-Pb(1)-O(10)	148.6(3)		
O(5)-Pb(2)-O(3)	155.9(3)		
N(1)-Pb(2)-O(8)	128.5(3)		

Symmetry codes: #1 –x, 1 – y, 1 – z; #2 –x + 2, y, – z + 3/2; #3 x, y – 1, z.

X-Ray diffraction analysis for complex **2** confirms that the asymmetric unit contains half a manganese ion, one 4,4′-bipy and two L ligands. Each manganese(II) centre is coordinated by two nitrogen atoms (N_1, N_2) from two 4,4′-bipy ligands and four oxygen atoms from the carboxylate of four L ligands, as shown in Fig. 5. In this complex, the Mn_1–O_3 interaction is weaker than the Mn_1–O_2 interaction because the Mn_1–O_3 bond length (2.201 Å) is longer than the Mn_1–O_2 bond length (2.132 Å). In this complex, each carboxyl of L, bridged two Mn ions. This connectivity pattern leads to infinite Mn–O–C rods (Secondry Building Units, SBU) along the *c*-axis direction (Fig. 6). Each rod is linked to two neighbouring rods by the 4,4′-bipy, resulting in a 2-D coordination layer along the *bc*-plane, as shown in Fig. 7. Like complex **1**, the π–π stacking interactions are formed between the adjacent benzene rings of different L ligands, which connect these 2-D coordination layers together in a 3-D, supermolecular, polymer (Fig. 8).

In both title supermolecular polymers, only C–H—X (X = O, N, Cl) interactions exist and no classical hydrogen bonds are presents. These van der Waals' forces increase the stabilization of

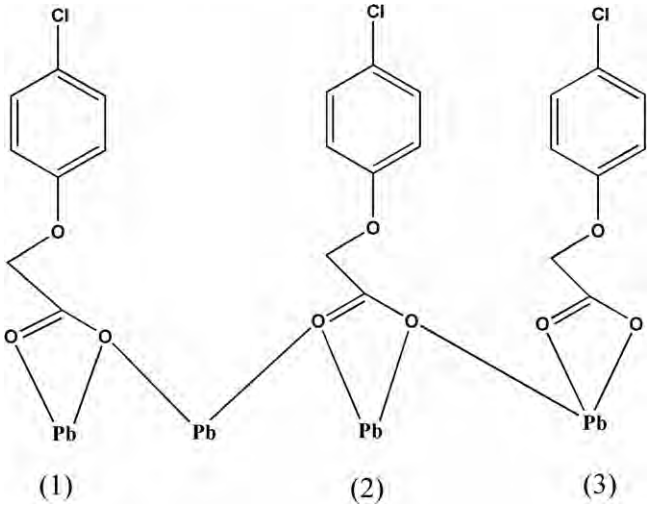

Scheme 1
Three possible coordination modes of L in complex **1**.

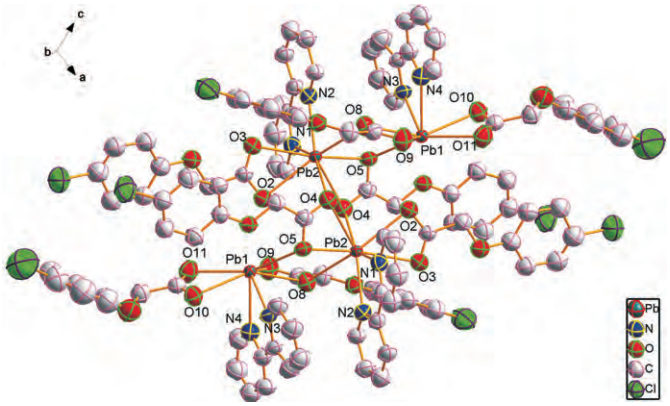

Figure 1 Ortep view of the coordination environment of **1**. All H atoms are omitted for clarity.

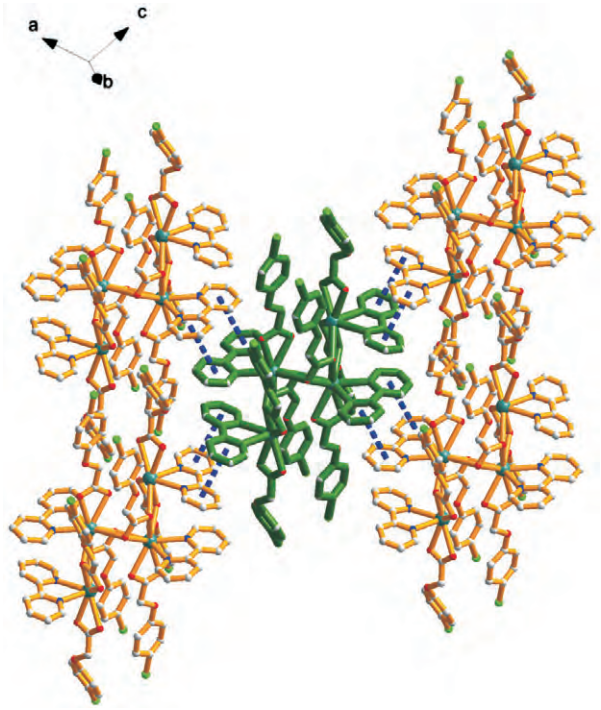

Figure 2 The face to face π-π stacking interactions between two pyridine rings of different 2,2′-bipy ligands in complex **1**; all H atoms are omitted for clarity.

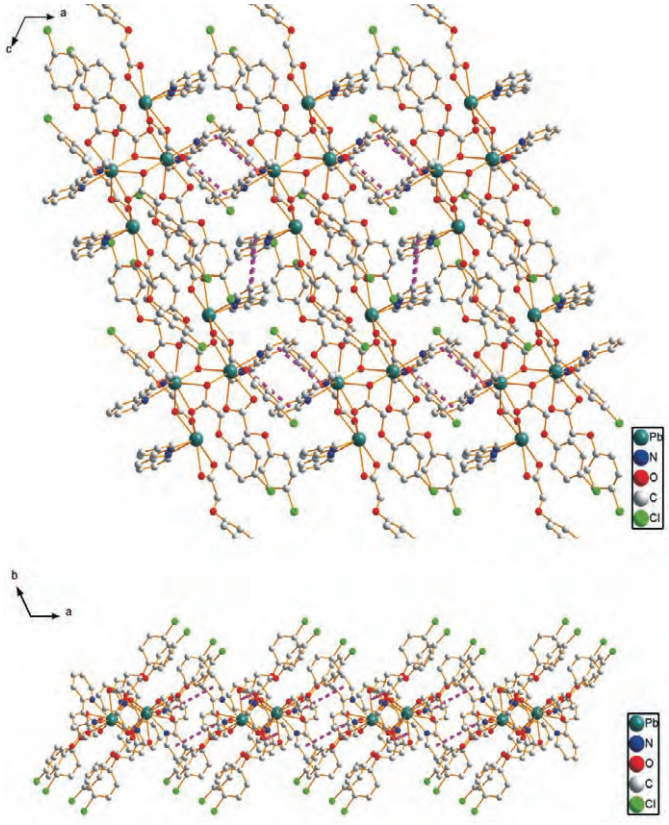

Figure 3 View of 2-D supermolecular layer in complex **1** along (top) the *b*-axis and (bottom) the *c*-axis; all H atoms are omitted for clarity.

the two supermolecular structures. Moreover, π–π stacking interactions also play an important role in stabilization of structures and extend the structures into 3-D supermolecular systems.

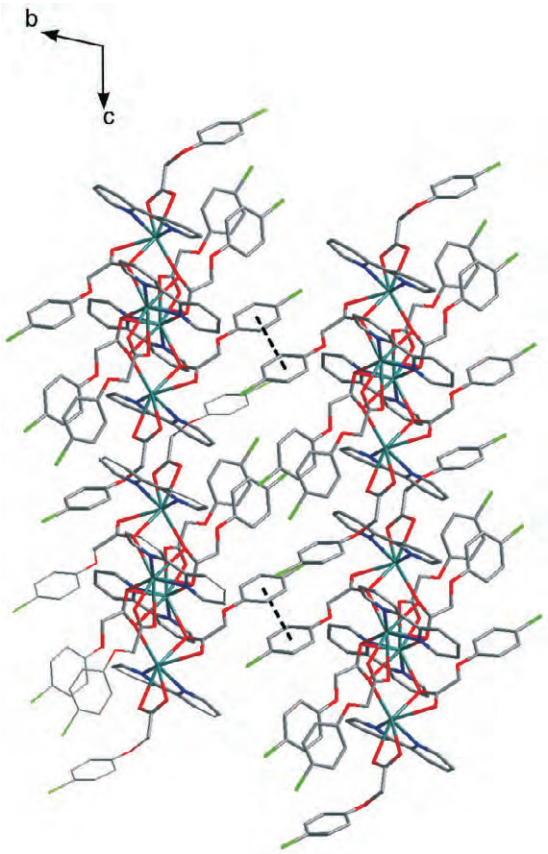

Figure 4 A part of the 3-D supermocelure structure of complex **1** formed by π–π stacking interactions.

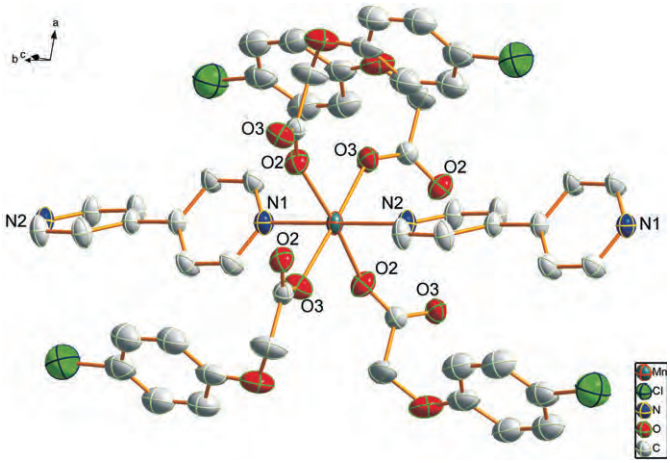

Figure 5 Ortep view of the coordination environment of **2**. All H atoms are omitted for clarity.

3.2. Fluorescence Properties

Complex **1** exhibits fluorescence emission around 326 nm and excitation at 303 nm in ethanol solution at room temperature (Fig. 9). The emission peak of complex **1** is neither metal-to-ligand charge transfer (MLCT) nor ligand-to-metal transfer (LMCT), since the Pb(II) ions, with an inert $6s^2$ electron pair are difficult to oxidize or reduce. This observation has been verified in the electrochemical test below. Therefore, the fluorescence is assigned to a π–π^* intra-ligand transition. Complex **2** shows two emission peaks: one at 384 nm and another at 325 nm when excited at 324 nm in ethanol solution at room temperature (Fig. 10). The major peak of complex **2**, which is dominated by

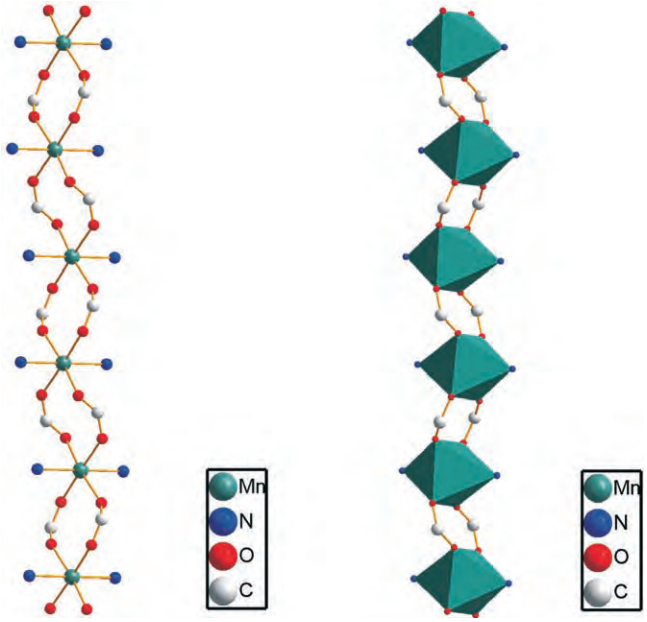

Figure 6 Infinite rod-shaped building blocks used to assemble 2-D layer in complex **2**: (left) ball-and-stick representation of SBU; (right) SBU shown as polyhedra.

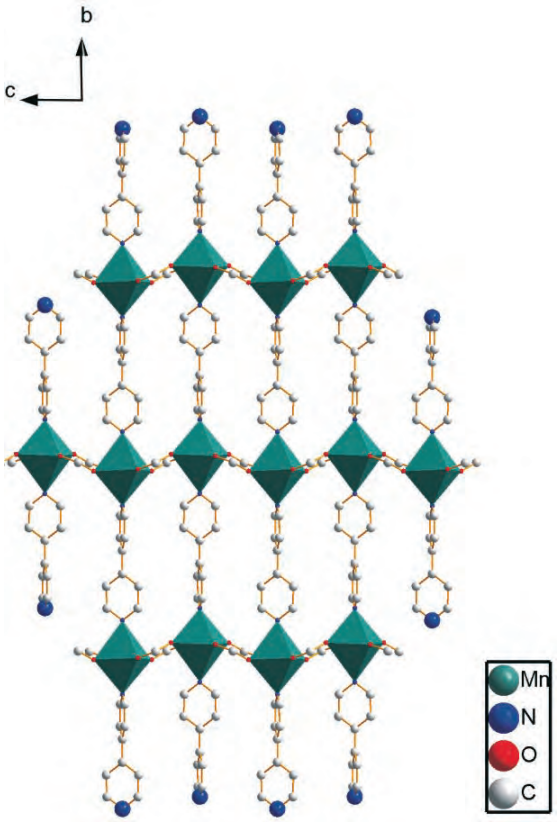

Figure 7 A perspective view of the 2-D coordination layer in complex **2** constructed by 4,4′-bipy .

π–π* type fluorescence, and the weak peak at 325 nm can be assigned to a ligand-to-metal charge transfer (LMCT) transition.

3.3. Electrochemical Properties

The electrochemical behaviour of complexes **1** and **2** in ethanol–water solution have been investigated by cyclic voltammetry in the potential range 0 to 1.6 V. Complex **1** shows no electrochemical properties, which corroborates that the Pb(II) ions

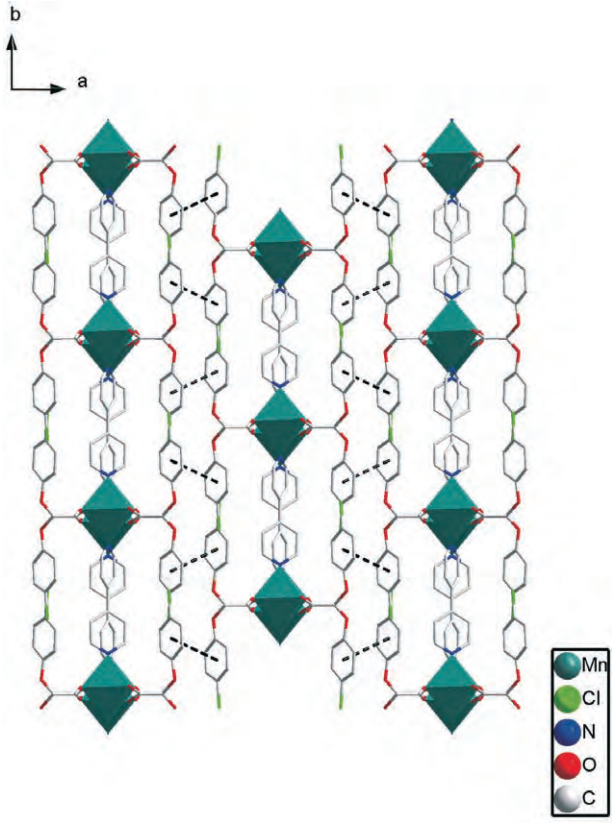

Figure 8 A part of the 3-D supermolecular structure made by π–π stacking interactions between the benzene rings of L ligands in complex **2**.

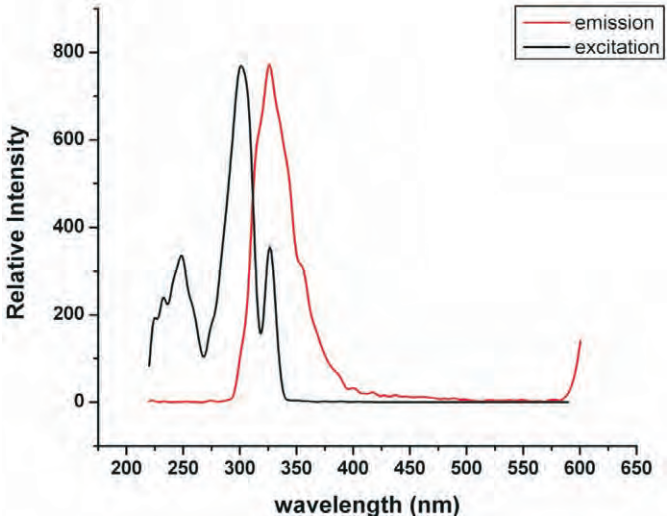

Figure 9 Emission spectrum and excitation spectrum of **1** in ethanol solution at room temperature.

are difficult to oxidize or reduce because of their $6s^2$ inert electron pair. Complex **2** displays two, quasi-reversible, oxidation and reduction waves, with a reduction potential ranging from 0.1 to 0.4 V and an oxidation potential ranging from 0.7 to 1.4 V (Fig. 11).

4. Conclusion

This paper reports the synthesis and characterization of complexes $[Pb_4L_8(2,2'\text{-bipy})_4]$ **1** and $[MnL_2(4,4'\text{-bipy})]$ **2** by fluorescence spectroscopy, electrochemical analysis, elemental

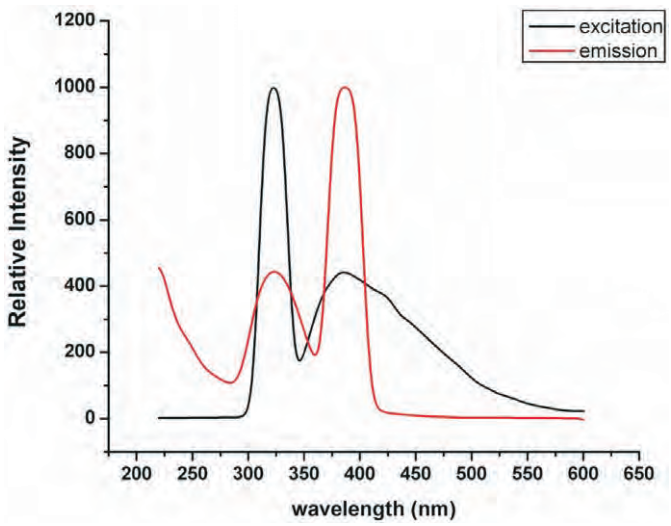

Figure 10 Emission spectrum and excitation spectrum of **2** in the ethanol solution at room temperature.

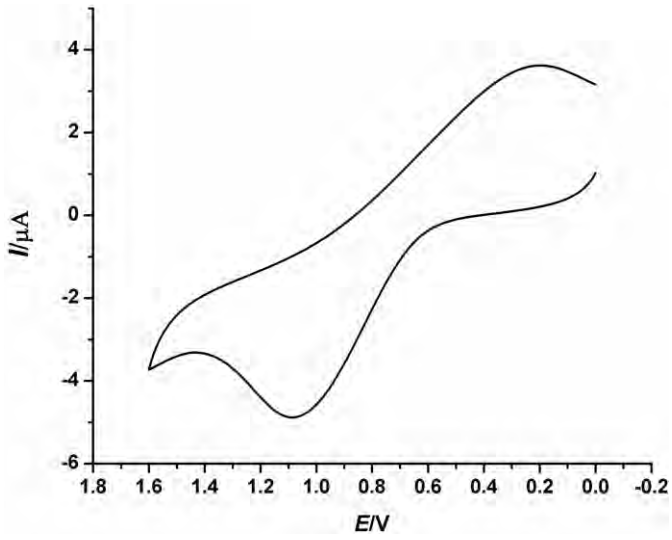

Figure 11 Cyclic voltammograms of complex **2** measured at room temperature.

analysis, and single-crystal X-ray diffraction techniques. The results show that the L ligand displays three kinds of coordination modes in complex **1** and only one mode in complex **2**. In complex **1**, four Pb ions linked together by eight L ligands in a dimer, in which π–π stacking interactions link these 2-D dimers together into a 3-D supermolecular polymer. In complex **2**, each carboxyl of L, bridg two Mn ions to form infinite Mn–O–C rods. π–π stacking interactions connect this 2-D structure into a 3-D supermolecular polymer. In both title complexes, there are van der Waals' forces that make the supermolecular polymers more stable. Both Complex **1** and Complex **2** exhibit fluorescence in methanol solution at room temperature. Complex **2** shows excellent electrochemical properties. Complex **1** displays no oxidation–reduction characterization due to the effect of its inert electron pair.

Acknowledgements

This work was financially supported by the Scientific Research Program of the Education Department of Guangxi Zhuang Autonomous Region (Project No. 201010LX081), and the Scientific Research Program of Guangxi University for Nationalities (Project No. 2010QD019).

References

1 J.L. Yang, E.S. Seong, M.J. Kim, B.K. Ghimire, W.H. Kang, C.Y. Yu and C.H. Li, *Plant Cell Tissue Organ Cult.* 2010, **42**, 49.
2 A.M. Castilla, T. Dauwe, I. Mora, J. Malone and R. Guitart, *Bull. Environ. Contam. Toxicol.* 2010, **66**, 101.
3 K. Ratanasanobon & K.A. Seaton, *Plant Cell Tissue Organ Cult.* 2010, **100**, 59.
4 S. Rakshit, Z. Rashid, J.C. Sekhar, T. Fatma and S. Dass, *Plant Cell Tissue Organ Cult.* 2010, **100**, 31.
5 L.L. Aylward, M.K. Morgan, T.E. Arbuckle, D.B. Barr, C.J. Burns, B.H. Alexander and S.M. Hays, *Environ. Health Perspect.* 2010, **118**, 177.
6 Y.X. Ren, B.J. Jiao, M.L. Zhang, X.M. Gao and J. Wang, *Z. Anorg. Allg.Chem.* 2011, **637**, 1612.
7 S.L. Fomulu, M.S. Hendi, R.E. Davis and K.A. Wheeler, *Cryst. Growth. Des.* 2002, **2**, 637.
8 C. Denderinou-Samara, G. Psomas, C.P. Raptopoulou and D.P. Kessissoglou, *J. Inorg. Biochem.*, 2001, **83**, 7.
9 Z.P. Li, Y.H. Xing, Y.Z. Cao, X.Q. Zeng, M.F. Ge and S.Y. Niu, *Polyhedron* 2009, **28**, 865.
10. G. Psomas, C. Dendrinou-Samara, P. Philippakopoulos, V. Tangoulis, C.P. Raptopoulou, E. Samaras and D.P. Kessissoglou, *Inorg. Chim. Acta.* 1998, **272**, 24.
11 D. Dougherty, *Science*, 1996, **271**, 163.
12 Q.Z. Chen, K., Cannell, J. Nicoll and D.V. Dearden, *J. Am. Chem. Soc.* 1996, **118**, 6335.
13 Blessing, R.H., *Acta Cryst. A*, 1995, **51**, 33.
14 G.M. Sheldrick, SHELXTL97, Program for refining crystal structure refinement, University of Göttingen, Germany, 1997.
15 B. Xu, Z.G. Guo, H.X. Yang, G.L. Li, T.F. Li and R. Cao, *J. Mol. Struct.* 2009, **922**, 140.
16 Y.X. Tan, F.Y. Meng, M.C. Wu and M.H. Zeng, *J. Mol. Struct.*, 2009, **928**, 176.
17 A. Ghosh, K.P. Rao, R.A. Sanguramath and C.N.R. Rao, *J. Mol. Struct.*, 2009, **927**, 37.

Supplementary material

CCDC 873690 and 873689 contain the supplementary crystallographic data for this paper. These data can be obtained free of charge *via* www.ccdc.cam.ac.uk/conts/retrieving.html (or from the Cambridge Crystallographic Data Centre, 12, Union Road, Cambridge CB2 1EZ, UK; fax: C44 1223 336033).